

SCIENTIFIC REPORTS



OPEN

Transcriptome analysis around the onset of strawberry fruit ripening uncovers an important role of oxidative phosphorylation in ripening

Qing-Hua Wang^{1,*}, Cheng Zhao^{1,*}, Miao Zhang^{2,*}, Yu-Zhong Li³, Yuan-Yue Shen¹ & Jia-Xuan Guo¹

Received: 06 May 2016
Accepted: 07 November 2016
Published: 14 February 2017

Although much progress has been made towards understanding the ripening of non-climacteric fruit using the strawberry as a model plant, the defined molecular mechanisms remain unclear. Here, RNA-sequencing was performed using four cDNA libraries around the onset of ripening, and a total of 31,793 unigenes and 335 pathways were annotated including the top five pathways, which were involved in ribosome, spliceosome, protein processing, plant-pathogen interaction and plant hormone signaling, and the important DEGs related to ripening were annotated to be mainly involved in protein translation and processing, sugar metabolism, energy metabolism, phytohormones, antioxidation, pigment and softening, especially finding a decreased trend of oxidative phosphorylation during red-coloring. VIGS-mediated downregulation of the pyruvate dehydrogenase gene *PDHE1 α* , a key gene for glycolysis-derived oxidative phosphorylation, could inhibit respiration and ATP biosynthesis, whilst promote the accumulation of sugar, ABA, ETH, and PA, ultimately accelerating the ripening. In conclusion, our results demonstrate that a set of metabolism transition occurred during green-to-white-to-red stages that are coupled with more-to-less DEGs, and the oxidative phosphorylation plays an important role in the regulation of ripening. On the basis of our results, we discuss an oxidative phosphorylation-based model underlying strawberry fruit ripening.

The ripening of fleshy fruit is a complex developmental process that involves many gene expression-controlled changes in texture, colour, flavour, and aroma. It is known that the process of climacteric fruit ripening is controlled by ethylene perception and signalling transduction¹. Although much progress has now been made towards understanding the ripening process for non-climacteric fruit through abscisic acid (ABA) metabolism and signaling in strawberries^{2–4} (*Fragaria ananassa*), the defined molecular mechanisms remain unclear.

The strawberry is an ideal model plant for the study of non-climacteric fruit ripening^{2,5}. In recent years, it is demonstrated that the ripening of strawberries is not only governed largely by ABA through a core signaling mechanism with the ABA-FaPYR1-FaPP2C-FaSnRK2 cascade^{2,6–12}, but also involved in several other plant hormones including brassinosteroids (BR)¹³, jasmonate (JA)¹⁴, ethylene (ETH)^{15,16}, and gibberellic acid (GA)¹⁷. Therefore, Shen and Rose (2015) consider that the regulation of non-climacteric ripening, to a large extent, is rather complex⁴.

Notably, transcriptional analyses of strawberries by expressed sequence tags (ESTs) and microarrays have found that ripening-related genes are involved in anthocyanin biosynthesis, cell wall degradation, sucrose and lipid metabolism, cellular transport, phosphatases, protein kinases, and transcription factors^{18–20}. These findings

¹Beijing Key Laboratory for Agricultural Application and New Technique, College of Plant Science and Technology, Beijing University of Agriculture, Beijing 102206, China. ²Beijing Yuanquanyike Biological Technology Company, Beijing 100197, China. ³Water Resources and Dryland Farming Laboratory, Institute of Agricultural Environment and Sustainable Development, Chinese Academy of Agricultural Sciences, Beijing 100081, P. R. China. *These authors contributed equally to this work. Correspondence and requests for materials should be addressed to Y.-Y.S. (email: sfrm@tom.com) or J.-X.G. (email: guojiaxuangjx@163.com)

have also been confirmed by proteomic analysis^{11,21}. MicroRNA analysis has indicated that NAC transcription factors, auxin response factors (ARF), and Myb transcription factors are also involved in the regulation of strawberry fruit ripening and senescence²². More importantly, numerous groups of genes related to fruit development have been identified. One such group comprises genes involved in ripening, including FaSHP¹⁰ (SHATTERPROOF-like, C-type MADS-box gene), FaMADS9²³ [A SEPALLATA(SEP)4-like gene], FaCDPK1²⁴ (a calcium-dependent protein kinase), an aldolase gene²⁵, FaCCD1²⁶ (a carotenoid cleavage dioxygenase class 1 enzyme gene), FaGAST1 and FaGAST2²⁷ (cysteine-rich domain proteins), and FaCAD1^{28,29} (cinnamyl alcohol dehydrogenase). Another group consists of the anthocyanin biosynthesis-related genes, including *FaMYB10*, *FaMYB1*, *FaPA*, *FaCHS*, *FaCHI*, *FaF3H*, *FaDFR*, *FaANS*, *FaUFGT*, and *FaPRX2*^{79,30–34}. A third group is the softening-related genes, which include *FaPG1*^{35,36}, *FaPL* and *FaPE1*^{37,38}, *FaEG1* and *FaEG3*^{39,40}, *FaRGLyase1*⁴¹, *FaXyl1*^{42,43}, *FaGAL1*⁴⁴, *FaEXP1*, *FaEXP2* and *FaEXP5*⁴⁵, and *FaPIP1* and *FaPIP2*^{46–48}. Finally, several genes related to volatiles have been identified, including *FaAAT1* and *FaAAT2*^{49–53}, *FaADH* and *FaPDC*⁵⁴, *FaOMT*^{55–57}, *FaNES1*⁵⁸, *FaFAD1*⁵⁹, *FaEGS1*⁶⁰, and *FaGT2*⁶¹.

The regulation of strawberry fruit ripening involves many phytohormones, transcription factors, cis-elements, and metabolic enzymes. This suggests that the ripening-regulated molecular mechanisms of non-climacteric fruit, in contrast to those of climacteric fruit regulated by ethylene, is highly complex. Given that one obvious sign of the onset of strawberry fruit ripening is the development of red colouration, transcriptome-based RNA sequencing carried out at the reddening stage may provide insight into the molecular mechanisms of non-climacteric fruit ripening. We constructed and sequenced the cDNA libraries of receptacles at the large green, white, initial-red and partial-red stages using the Illumina HiSeq 2000 platform. Based on our results, we outline an oxidative phosphorylation-based model for the onset of strawberry fruit ripening.

Results

RNA sequencing analysis and de novo assembly. To maximize the transcriptional data obtained from ripening strawberries, we prepared four mixed cDNA libraries from ten uniformly sized fruits at each of four stages of ripeness for RNA sequencing using the Illumina HiSeq 2000 instrument⁶². Each sequenced sample yielded 100 bp reads from paired-end sequencing of cDNA fragments. After quality assessment and data clearance, 5.58–7.71 billion (G) reads with more than 90% Q20 bases (i.e., an average base quality greater than 20) were retained as high-quality reads for each library and used in subsequent analyses (Supplemental Table 1). The average ‘G + C’ content of the above was 48% [46%, 50%, 49%, and 48% for CM1 (large green), CM2 (white), CM3 (initial-red), and CM4 (partial-red) libraries, respectively] (Supplemental Table 1).

All valid reads were combined to perform de novo assembly by the paired-end method with Trinity software⁶³ (trinityrnaseq_r20131110 version). A total of 98,848 unigenes were obtained, among which 24,358 genes were longer than 1 kb. An overview of the assembled transcripts and unigenes are presented in Supplemental Table 2. The length distributions of unigenes are shown in Supplemental Figure 1. These results demonstrate the effectiveness of Illumina pyrosequencing in rapidly capturing a large portion of the transcriptome.

Sequence annotation. We used several complementary approaches to annotate the assembled sequences. The unigenes were compared against diverse protein databases, including the National Center for Biotechnology Information (NCBI) non-redundant protein (NR) database, SWISS-PROT, TrEMBL, Cdd, pfam, KOG database, Kyoto Encyclopedia of Genes and Genomes (KEGG), and Gene Ontology (GO). The resulting functional annotations are listed in Supplemental Table 3 and provide the best unigenes with an E-value of $1e^{-5}$ and identity of 30%. We performed a sequence similarity search against the NCBI NR and SWISS-PROT protein databases using the Basic Local Alignment Search Tool (BLAST) algorithm, specifying an E-value of less than $1e^{-5}$. This analysis indicated that of the 98,848 unigenes, 41,282 (41.76%) matched the NR database and 25,312 (25.61%) had similarity to proteins in the SWISS-PROT database. A total of 14,267 unigenes classified into 25 KOG annotations are provided in Supplemental Figure 2. The top three functional categories were signal transduction mechanisms, posttranslational modification/protein turnover/chaperones, and general function prediction only. Altogether, 43,769 (44.3%) unigenes were successfully annotated in NR, SWISS-PORT, TrEMBL, Cdd, pfam, KOG, KEGG, and GO. The high percentage (55.7%) of unmapped unigenes that could be assigned a putative function may be due mainly to the short sequence reads generated by the sequencing technology and the relatively short sequences of the resulting unigenes, most of which probably lack the conserved functional domains. Another possible explanation may be that some unigenes were non-coding RNAs or unknown.

Based on the BLAST UniProt annotation, we carried out GO analysis, which led to the annotation of 31,793 unigenes. The results comprise three classifications: “biological process,” “cellular component,” and “molecular function.” The most frequently associated GO terms for the biological process group were “metabolic process” (GO:) and “cellular process” (GO:); for the cellular component group, they were “cell” (GO:) and “cell part”; and for the molecular function group they were “binding” (GO:0005488) and “catalytic activity” (GO:0003824) (Supplemental Figure 3).

To analyze the KEGG pathway of unigenes, we used KAAS to obtain corresponding KO numbers. These KO numbers were then used to obtain corresponding KEGG pathways. By analysing the relationship between unigenes and enzymes in KEGG comment files and mapping them to the pathway, we created 335 pathway charts. This process predicted a total of 301 pathways represented by a total of 14,011 unigenes (Supplemental Table 4). The top five pathways were involved in ribosomes, spliceosomes, protein processing, plant-pathogen interaction, and plant hormone signal transduction (Supplemental Table 5).

Gene expression patterns throughout fruit development. We used the distribution of gene expression levels to evaluate the normality of the library data. Gene expression level was determined by calculating the number of reads and normalising to the RPKM. As shown in Fig. 1, the majority of mRNAs were expressed at low

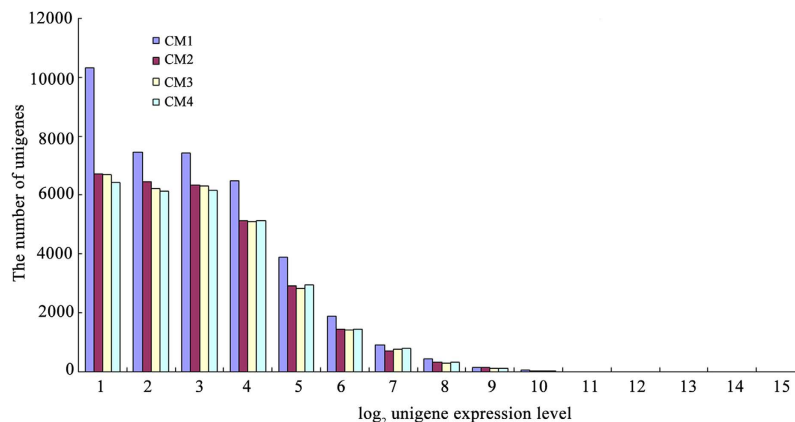


Figure 1. The distribution of gene expression levels. Total unigenes from each of four libraries were plotted as integrated log₂ gene expression category.

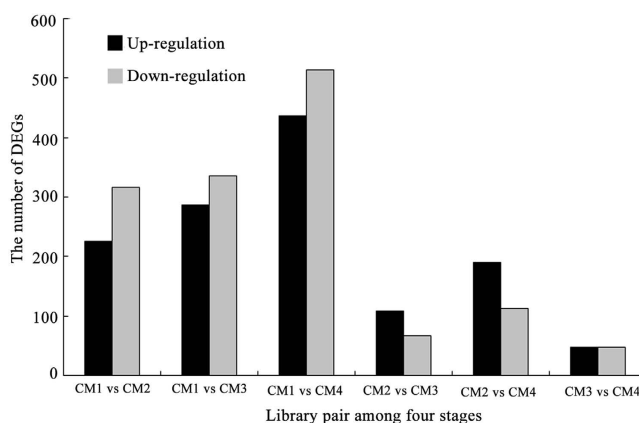


Figure 2. Differently expressed genes (DEGs) among the four-stage fruit. The number of up/down-regulated DEGs genes between library pairs was summarized by NCBI-NR, SWISS-PROT, TrEMBL, Cdd, pfam, KOG, KEGG and GO databases.

levels, whereas a small proportion was highly expressed. In CM1, most genes (10,307) have expression levels close to 1 (<1 , namely log₂ [2 RPKM]), while only 0.07% of the genes (27 of 39,086) were highly expressed at a level above 10. Compared with CM1, the distribution of the CM2, CM3, and CM4 libraries showed similar expression patterns; in other words, the later stages (white, initial-red, partial-red) were distinct from the large green stage, suggesting that the white stage might represent the onset of fruit ripening.

To analyze variation in gene expression throughout strawberry fruit development, the differentially expressed genes (DEGs) between each library pair (CM1-CM2, CM1-CM3, CM1-CM4, CM2-CM3, CM2-CM4, and CM3-CM4) were listed in Fig. 2. The results showed that more DEGs were detected when comparing CM2-CM4 to CM1, and among these DEGs, downregulated genes were predominant, indicating that the onset of fruit ripening is coupled with many genes that were downregulated. Comparing CM3/CM4 with CM2, DEGs decreased sharply and upregulated genes were predominant, showing that these upregulated genes may therefore be involved in the onset of ripening. Notably, CM3 and CM4 had similar gene expression patterns. Some important DEGs related to ripening were listed in the Heatmap Fig. 3, mainly included oxidative phosphorylation (NADH, ATPase), plant hormones (ABA, IAA, GA, ETH, JA and PA), antioxidation (GST, Vc), protein translation and processing, sugar metabolism, pigment and softening. Taken together, these results suggest that a set of metabolism transition occurred during green-to-white-to-red stages, and the processes of fruit de-greening are more complex than those of fruit red-colouring, and that white fruit is a distinct stage.

Enrichment pathway analysis of DEGs. We performed KEGG pathway enrichment analysis to categorise the biological functions of DEGs. We mapped all the genes to terms in the KEGG database. Comparing CM1 with CM2, CM3, and CM4, 41, 52, and 54 pathways were upregulated while 42, 48, and 54 pathways were downregulated, respectively. Comparing CM2 with CM3 and CM4, 36 and 39 pathways were upregulated while 42 and 43 pathways were downregulated, respectively. Comparing CM3 with CM4, 27 pathways were upregulated while 30 pathways were downregulated. Some DEGs specific to each stage are listed in Fig. 4, compared CM2/CM3/CM4 with CM1, 828, 930 and 1312 DEGs were found, respectively (Fig. 4A); compared CM3/CM4 with CM2, 284 and 483 DEGs were found, respectively (Fig. 4B); compared CM4 with CM3, only 192 DEGs were found.

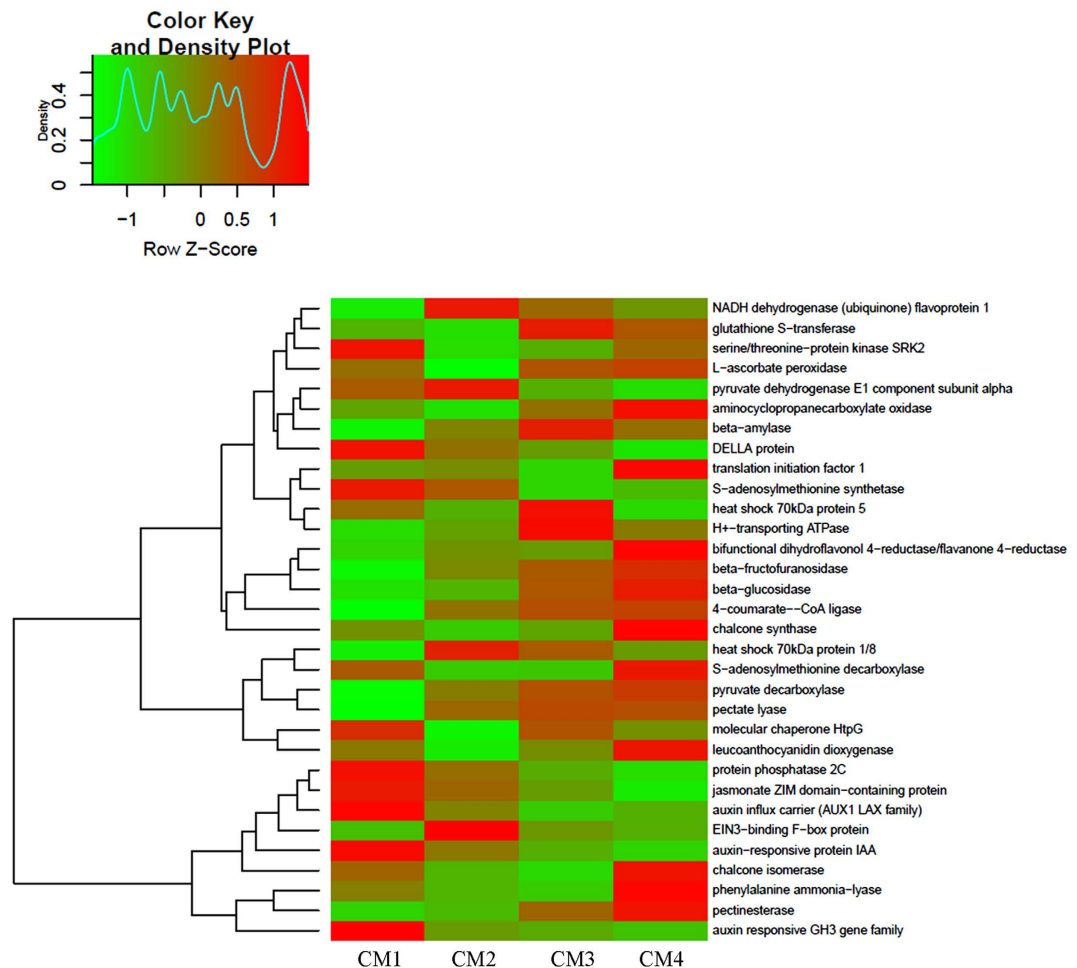


Figure 3. The Heatmap and cluster analysis of transcripts for the important genes related to the fruit ripening. Data for gene expression levels were normalized to z-score with the formula $\log_{10}(\text{FPKM} + 1)$ by color key and density plot, namely, the from-green-to-red color represents the value of gene expression from low to high during fruit ripening. The gene-coding proteins annotated in the relative pathways: **oxidative phosphorylation** [NADH dehydrogenase (ubiquinone) flavoprotein 1, H⁺-transporting ATPase]; **glutathione metabolism** [glutathione S-transferase (GST), L-ascorbate peroxidase (Vc)]; **abscisic acid** [ABA, serine/threonine-protein kinase SRK2, protein phosphatase 2C (PP2C)]; **protein processing** (heat shock 70 kDa protein 5, heat shock 70 kDa protein 1/8, molecular chaperone HtpG); **RNA transport** (translation initiation factor 1); **sugar metabolism** [pyruvate dehydrogenase E1 component alpha (PDH), beta-amylase, beta-fructofuranosidase, beta-glucosidase, pyruvate decarboxylase (PDC)]; **ethylene** [ETH, aminocyclopropanecarboxylate oxidase (ACO), EIN3-binding F-box protein (EBF), S-adenosylmethionine synthetase (SAMS)]; **Gibbérilline** (GA, DELLA protein); **flavonoid biosynthesis** [bifunctional dihydroflavonol 4-reductase/flavanone 4-reductase (DFR), chalcone synthase (CHS), chalcone isomerase (CHI), leucoanthocyanidin dioxygenase (LDOX), naringenin 3-dioxygenase (FHT)]; **phenylpropanoid biosynthesis** [4-coumarate-CoA ligase (4CL)], beta-glucosidase, phenylalanine ammonia-lyase (PAL)]; **pentose and glucuronate interconversions** [pectinesterase (PE), pectate lyase (PL)]; **jasmonate** [JA, jasmonate ZIM domain-containing protein (JAZ)]; **auxin** (IAA, auxin-responsive protein IAA, auxin influx carrier, auxin responsive GH3 gene family); **polyamines** [PA, S-adenosylmethionine decarboxylase (SAMDC)].

The ten most DEG-rich pathways between library pairs are provided in Supplementary Table 6. Between CM1 and CM2, protein turnover and processing increased within pulp cells, as well as including oxidative phosphorylation, carbohydrate metabolism and the plant hormones (ABA, JA). The carbohydrate metabolism pathways included carbon fixation, glycolysis/gluconeogenesis, pentose and glucuronate interconversions, as well as starch degradation, sucrose accumulation, amino sugar, and nucleotide sugar metabolism related to fruit softening. Meanwhile, DNA turnover, photosynthesis, cell cycle, emergency reactions, and the plant hormones (IAA, GA, ETH and PA) signaling decreased within pulp cells.

Between CM1 and CM3/CM4, pulp cells maintained high levels of protein turnover and processing, oxidative phosphorylation, carbohydrate metabolism and the plant hormones (ABA, JA). Glutathione, phenylpropanoid/flavonoid, cysteine, and methionine metabolism were also active. Notably, cysteine and methionine metabolism were involved in ETH and PA biosynthesis. Carbon fixation, starch degradation, plant-pathogen reaction, and

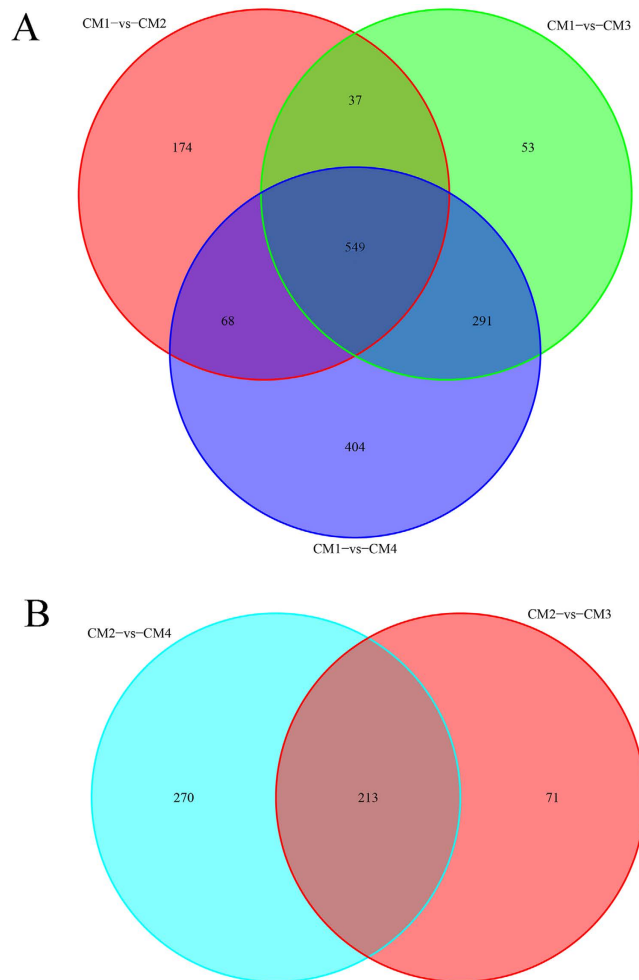


Figure 4. A Venn diagram for the different DEGs between each-stage-library pair. (A) Comparing CM2/CM3/CM4 to CM1; (B) Comparing CM3/CM4 to CM2.

glyoxylate and dicarboxylate metabolism, and the plant hormones (including IAA and GA) signal transduction decreased.

Comparing CM2 to CM3/CM4, pulp cells sustained high levels of protein/DNA/RNA turnover and processing, as well as glutathione, flavonoid, sucrose metabolism and the plant hormones (ABA, JA, ETH and PA). Meanwhile, photosynthesis, carbon fixation, and the plant hormone (GA and IAA) signal transduction, as well as cysteine, methionine, and starch metabolism, decreased. Notably, oxidative phosphorylation metabolism also decreased.

Comparing CM3 to CM4, pulp cells sustained high levels of phenylpropanoid/flavonoid biosynthesis, carbohydrate metabolism (involved in pectate lyase, pectinesterase and beta-glucosidase), cysteine and methionine metabolism and the plant hormones (ABA, JA, ETH and PA). Porphyrin and chlorophyll metabolism, related to chlorophyll degradation, were also sustained at high levels. Photosynthesis, carbon fixation, and the plant hormone (GA and IAA) signal transduction decreased, as well as starch metabolism and oxidative phosphorylation.

Together, these results show that the processes of strawberry fruit ripening involve a decrease in oxidative phosphorylation and the plant hormone (GA and IAA) signaling, while an increase in carbohydrate, phenylpropanoid, flavonoid, glutathione, methionine and the plant hormone (ABA, JA, ethylene, and PA) signaling. The fact that the oxidative phosphorylation decreases at red-coloring, suggests a regulatory role of oxidative phosphorylation in ripening.

Downregulation of PDHE1 α by VIGS promotes strawberry fruit red-colouring. Given that the white stage represents the onset of fruit ripening and only several genes have an increased expression in this staged, including NADH dehydrogenase (ubiquinone) flavoprotein 1, pyruvate dehydrogenase E1 component alpha, heat shock 70 kDa protein 1/8 and EIN3-binding F-box protein (Fig. 3). It is known that pyruvate dehydrogenase contributes to linking the glycolysis metabolic pathway with the citric acid cycle and releasing energy via NADH dehydrogenase-mediated oxidative phosphorylation, and its E1 subunit is considered to be the rate-limiting step for the pyruvate dehydrogenase⁶⁴.

To further explore the role of oxidative phosphorylation in strawberry fruit development, we used the transcriptome data to investigate the mRNA expression levels of pyruvate dehydrogenase. The results showed that the

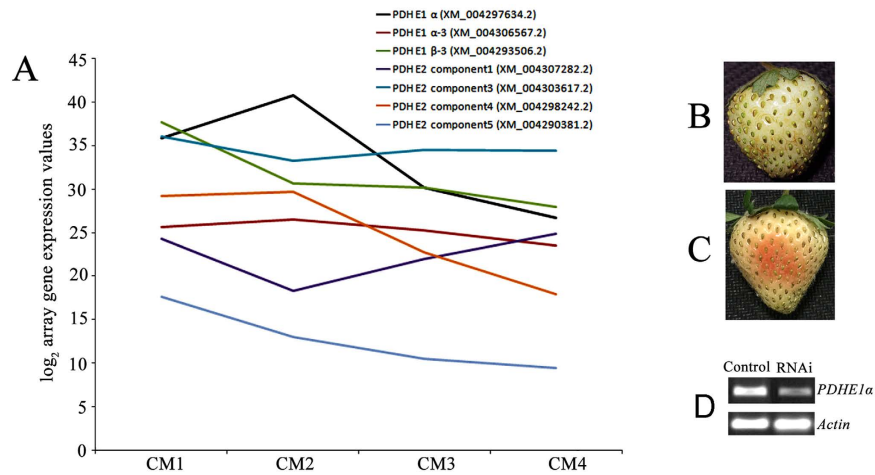


Figure 5. RNA-seencing analysis of pyruvate dehydrogenase gene family and silencing of *PDHE1α* by VIGS in the fruit. (A) RNA-seencing analysis of pyruvate dehydrogenase gene family. (B,C) Twenty large green fruit were used for treatment and control tests, respectively. One week after inoculation, phenotypes were observed for the control fruit (B) and RNAi fruit (C), respectively. (D) SqRT-PCR analysis of the transcripts of *PDHE1α* in receptacles of control fruit and RNAi fruit. *Actin* was used as a reference gene.

E1 component subunit alpha of pyruvate dehydrogenase gene, *PDHE1α* (GenBank NO. XM_004297634.2), had an increased expression in white stage, and then followed a high-to-low pattern during strawberry fruit ripening (Fig. 5A). In order to investigate a role of the *PDHE1α* in the fruit ripening, the *PDHE1α* gene expression was silenced using syringe-infiltrated a mixture of *Agrobacterium* strain GV3101 cultures containing pTRV1 and pTRV2 carrying a 589-bp fragment of the gene (pTRV2-*PDHE1α*) into large green fruit in a 1:1 ratio. Control fruits were infiltrated only with TRVs alone. One week after infiltration, control fruit remained white (Fig. 5B); in contrast, RNAi fruit turned red (Fig. 5C), and *PDHE1α* transcripts were downregulated compared to the control (Fig. 5D). The results that downregulation of *PDHE1α* expression stimulated the fruit ripening, making *PDHE1α* a negative regulator of strawberry fruit ripening.

Alteration of *PDHE1α* expression affects the ripening-related physiological parameters. To further elucidate the role of *PDHE1α* in the regulation of strawberry fruit ripening, we assayed ripening-related physiological parameters in both RNAi and control fruit, including plant hormones (ABA, GA, IAA, JA, ETH, and PA), soluble solids (sugar) concentration, biochemical measurements of oxidative phosphorylation (ATP), and respiration rate. The levels of ABA, ETH, PA, and soluble solids concentration were all remarkably high in RNAi fruit compared with control fruit (Table 1). In contrast, the levels of IAA, GA₃, and JA showed non-significant changes between the RNAi and control fruit. Notably, both ATP content and respiration rate were markedly lower in RNAi fruit compared with control fruit. These results suggest that downregulation of *PDHE1α* expression inhibits respiration and ATP biosynthesis, resulting in an increase in soluble solids concentration and an accumulation of ABA, ETH, and PA, which ultimately promotes the ripening in RNAi fruit.

Discussion

While the molecular mechanisms of strawberry fruit ripening are highly complex, the external signs (de-greening and red-colouring) are very simple. On the basis of our transcriptome-based RNA-seencing analysis around the onset of ripening using large green, white, initial-red, and partial-red fruit, the previous and our data indicate that the pyruvate dehydrogenase E1α (PDHA1) is the first component enzyme of the pyruvate dehydrogenase (PDH) complex that catalyzes the overall conversion of pyruvate to acetyl-CoA, which is subsequently used in cellular respiration by both the citric acid cycle and oxidative phosphorylation to generate ATP, so this E1α subunit is considered to be the rate-limiting step for the pyruvate dehydrogenase complex^{64,65}. The downregulation of *PDHE1α* expression inhibits respiration, ATP biosynthesis, and ABA and ETH accumulation (Fig. 5 and Table 1), to some extent, suggesting that a link between oxidative phosphorylation and strawberry fruit ripening is existed. Further explain is as follows:

It is known that oxidative phosphorylation play a central role in supplying the carbon skeleton and motive force for biochemical reactions, and that pyruvate dehydrogenase is a key step in the oxidative phosphorylation stage of sugar metabolism⁶⁶. Our RNA-seencing analysis indicated that the mRNA expression level of the E1 component subunit alpha of the pyruvate dehydrogenase gene *PDHE1α* follows a trend similar to that of oxidative phosphorylation activity at the onset of strawberry fruit ripening (Fig. 5). Interestingly, the downregulation of *PDHE1α* expression could inhibit respiration and ATP biosynthesis, whilst also promoting the accumulation of sugar, ABA, ETH, and PA, ultimately accelerating fruit ripening (Table 1). These results are consistent with previous reports on the roles of ABA, ETH, and sugar in the regulation of strawberry fruit ripening^{2,7-12,67,68}.

On the one hand, glycolysis-derived oxidative phosphorylation provides the required carbon and energy fluxes for fruit development; on the other, cellular respiration through oxidative phosphorylation exhausts carbohydrates that provide the basis for fruit development. In the present study, the number of the differentially

Fruit	ABA (ng/g FW)	GA (ng/g FW)	IAA (ng/g FW)	JA (ng/g FW)	PAs ($\mu\text{g/g FW}$)	ETH ($\mu\text{L/kg h FW}$)	Solid soluble concentrations (g/100 g FW)	ATP ($\mu\text{g/g FW}$)	Respiration rate (mg/kg h)
RNAi	135.27 \pm 9.20	11.15 \pm 1.72	90.82 \pm 7.31	24.17 \pm 3.82	79.31 \pm 5.51	0.28 \pm 0.07	6.78 \pm 1.03	17.05 \pm 1.83	11.29 \pm 1.54
	b	a	a	a	b	b	b	a	a
WT	109.34 \pm 8.93	10.60 \pm 1.13	87.95 \pm 6.73	25.94 \pm 2.59	55.45 \pm 4.02	0.16 \pm 0.04	4.53 \pm 0.71	29.24 \pm 2.58	19.06 \pm 2.35
	a	a	a	a	a	a	a	b	b

Table 1. Downregulation of *PDHE1 α* expression affects the ripening-related physiological parameters.

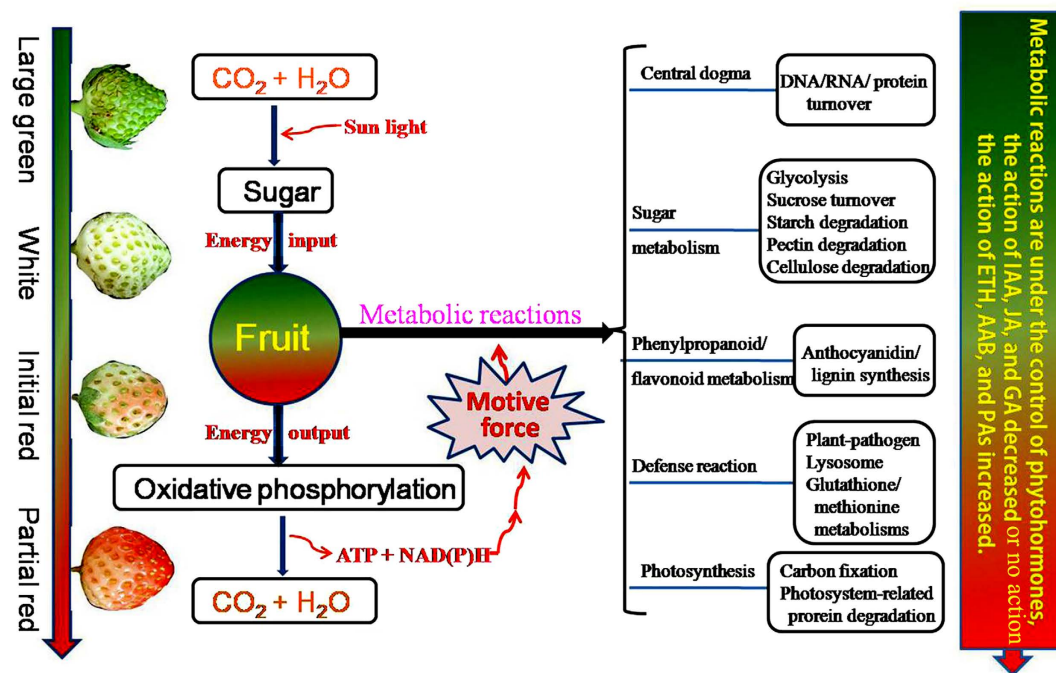


Figure 6. A model for the processes of strawberry fruit ripening at molecular level. With the action of sun energy, CO_2 and H_2O can be transformed into sugar by photosynthesis in chloroplast of leaves and fruit, the sugar can be turned into CO_2 and H_2O by oxidative phosphorylation to produce the motive force [ATP and NADH] for metabolic reactions. Coupled with the fruit de-greening and red-coloring, protein/DNA/RNA turnover always follows, the increased-sugar metabolisms are involved in glycolysis, sucrose turnover, and starch, pectin and cellulose; the increased-phenylpropanoid/flavonoid metabolisms are mainly involved in anthocyanidin and lignin synthesis; The defense reactions are involved in plant-pathogen interaction, lysosome, glutathione, and methionine metabolisms. The cellular global metabolisms are under the programmed regulation of plant hormones, the action of IAA, JA, and GA decreased while the action of ethylene, ABA, and PA increased.

expressed genes (DEGs) is remarkable lower after white stage (comparing CM3/CM4 with CM2) in comparison to de-greening stages (comparing CM3/CM4/CM2 with CM1; Fig. 2, Supplemental Table 6), suggesting that the processes of early development are more complex (more DEGs) before white stages, once on the set of red-coloring in white fruit, the processes of ripening is relative simple (less DEGs). To a large extent, a metabolism transition occurred during green-to-white-to-red stages. In response to this change, fruit decreased oxidative phosphorylation intensity, which in turn promoted the accumulation of sugar, ABA, and ETH (Table 1), which can accelerate fruit ripening^{7,67}.

On the basis of the available data, we have tentatively outlined the processes of strawberry fruit ripening at the molecular level. With the action of sun energy, CO_2 and H_2O can be transformed into sugar by carbon fixation in the chloroplasts of leaves and fruit. Sugar can be turned into CO_2 and H_2O by oxidative phosphorylation in order to produce the motive force for biochemical metabolic reactions in fruit. During fruit development, protein/DNA/RNA turnover and oxidative phosphorylation follow a decreasing trend that corresponds to DEG variation (Fig. 2 and Table 1). It is interesting to note that, most upregulated DEGs were involved in sugar accumulation, fruit softening, and pigment biosynthesis (phenylpropanoid/flavonoid metabolism), while the capacity of fruit for carbon fixation and resistance decreased (Fig. 3 and Table 1). In response to these changes, fruit cells accelerate lysosome action and evoke cellular antioxidant action through glutathione and methionine metabolism^{20,69}. Undoubtedly, cellular metabolism is regulated by plant hormones in response to fruit developmental cues: coupled with the onset of the fruit ripening, the action of ABA, ethylene, and polyamine increased (Fig. 6).

The present study provides the first description of an oxidative phosphorylation-based model for strawberry fruit ripening based on transcriptome data. Given the complexity of non-climacteric fruit ripening, the roles of aerobic respiration and anaerobic respiration in the regulation of fruit ripening are subjects for future study.

Materials and Methods

Plant material. Octoploid strawberry (*Fragaria × ananassa* cv. Hongyan) plants were grown in a greenhouse (17–26 °C, relative humidity 70–90%, 14/10-h light/dark regime) in springtime during 2013–2014. Sixty flowers on 20 strawberry plants were tagged during flowering. Four fruit stages (large green, white, initial-red, and partial-red) were numbered from CM1 to CM4 and collected at 18, 24, 27, and 29 days after anthesis, respectively. Ten uniformly sized fruits were sampled at every stage (one replicate). After removing the achenes (seeds), the receptacle (pulp) was cut into 0.5–0.8 cm³ cubes and quickly stored in liquid nitrogen.

RNA extraction, library construction, and RNA-seq. Three fruits were randomly taken out from the frozen samples for every RNA isolation and cDNA synthesis. RNA was extracted using the RNeasy plant mini kit (Qiagen, Dusseldorf, Germany) from the receptacles of CM1–CM4 fruit. DNase digestion with the RNase-Free DNase set (Qiagen) was performed to remove contaminating DNA, and the RNA samples were then processed using the RNA library prep kit (New England Biolabs, Ipswich, MA, USA) and sequenced with the Illumina HiSeq2000 platform. The experiments were repeated three times.

Sequence data analysis and assembly. The raw reads were filtered with the FASTQ_Quality_Filter tool from the FASTX-toolkit. Reads with more than 35 bp having a quality score higher than 20 were kept⁷⁰. All valid reads were combined to perform de novo splicing by the paired-end method with Trinity software⁷¹. The longest transcripts per locus were used as a unigene.

Functional annotation. Several complementary approaches were utilised to annotate the unigenes. Searches were conducted using the Basic Local Alignment Search Tool (BLASTX)⁷². The unigenes were compared against the NCBI NR, SWISS-PROT, TrEMBL, Cdd, pfam, and KOG databases with an E-value of 1e-5 and identity of 30%⁷³. Functional annotation by gene ontology terms (GO, <http://www.geneontology.org>) was carried out using the Blast2GO software^{74,75}. To achieve KEGG orthology (KO) assignment⁷⁶, the Kyoto Encyclopedia of Genes and Genomes (KEGG) pathways were assigned to sequences using the online KEGG Automatic Annotation Server (KAAS) (<http://www.genome.jp/kegg/kaas/>)^{77,78}. The output of KEGG analysis includes KO assignments and KEGG pathways^{77,78}.

The bowtie2–2.2.2 software was used to compare reads with unigenes using the single-end mapping method^{71,79}. To compare the levels of unigene expression among the four libraries, the transcript level of each expressed unigene was calculated and normalised to the reads per kilobase of the exon model per million mapped reads⁸⁰ (RPKM). The significance of differential unigene expression was determined by using the Chi-squared test with a threshold of $P = 0.05$. P-values were adjusted to account for multiple testing by using the false discovery rate (FDR) and assigned error ratio Q-values (< 0.05)⁸¹. The unigenes with an adjusted P-value of < 0.05 and an absolute value of \log_2 (expression fold change) > 1 were deemed to be differentially expressed, while the unigenes with an FDR-adjusted P-value of < 0.05 were considered statistically significant.

VIGS and SqRT-PCR analysis. Following the method of Jia *et al.*⁷ (2011), a 589-bp cDNA fragment of *PDHE1α* was amplified using primers (sense 5'-TCTAGAACCACTGCACCTTCCTCG-3', underlined is *Xba* I, and antisense 5'-CTCGAGTACGCTCCTG TCTCACG-3', underlined is *Xho* I) cloned into the virus vector *Xba* I-*Xho* I-cut pTRV2. *Agrobacterium* strain GV3101 containing the pTRV1, pTRV2, or pTRV2 derivatives pTRV2-PDHE1 α ₅₈₉ was used for RNAi (Fig. 5). *Agrobacterium*-mediated TRV infiltration by syringe injection with a needle into strawberry fruits was performed as described by Jia *et al.*⁷ (2011). For semi-quantitative RT-PCR (SqRT-PCR) analysis of *PDHE1α* transcripts, the cDNA was used as a template for PCR amplification through 25 cycles and actin was used as a reference gene (sense 5'-CAGTTAGGAGAACTGGGTGC-3' and antisense 5'-TGGGTTTGCTGGAGATGAT-3'). The experiments were repeated three times.

Determination of fruit respiration, ethylene release rate, and soluble solid content. 200 g of fruit were sealed in a 500 mL glass bottle at 25 °C. After 1 h, 10 mL of gas sample were used to measure respiration rate with an infrared carbon dioxide analyser (AMETEKMode ICD-3A) and ethylene release rate with a HP P5890a gas chromatograph. The soluble solids content of flesh was measured using a hand-held sugar measurement instrument (MASTER-100H, ATAGO Master, Japan), onto which fruit juice was applied to obtain a reading. Ten uniformly sized fruit were used for analysis. The experiments were repeated three times.

ATP assay. ATP synthesis rates were measured using a luminometer (Glomax 96 Microplate Luminometer; Promega). 20 mL of isolated pulp chromoplasts were added to microplate wells containing 80 mL of luciferase/luciferin reagent (ENLITEN; Promega) and 80 mL of buffer (600 mM sorbitol, 10 mM TES, 2 mM MgCl₂, 25 mM KH₂PO₄, and 0.33 mM EDTA, pH 7.4). Ten uniformly sized fruit were used for ATP synthesis measurement, and the experiments were repeated three times.

Hormone analysis. In order to determine ABA, IAA, GA, and JA contents, 0.5 g receptacle samples were ground in a mortar and homogenised in extraction solution (80% methanol, v/v). Extracts were centrifuged at 10,000 × g for 20 min. The supernatant liquid was eluted through a Sep-Pak C18 cartridge (Waters, Milford, MA, USA) to remove polar compounds, and then stored at –20 °C for enzyme-linked immunosorbent assay (ELISA) according to the manufacturer's instructions (China Agricultural University, Beijing, China). Ten uniformly sized fruit were used for detection, and the experiments were repeated three times.

Polyamines assay. The polyamines assay was performed using high performance liquid chromatography (HPLC) with the Waters™ 996 photodiode Array Detector, Millennium 32 Chromatography software, and Diamond C18 columns (250 × 4.6 mm, 5 μm). The wavelength of detection was 230 nm, the flow rate was 1.2 mL/min, and the mobile phase was acetonitrile:methanol:water (3:4:3, v-v:v). 3 mL of precooled 5% perchloric acid (V/V) were added to 1 g samples, and the mixture was ground to homogeneity at 4 °C and centrifuged (15,000 rpm, 30 min, 4 °C) after 1 h extraction. 1 mL of supernatant, 7 μL of benzoyl chloride, and 1 mL 2 M NaOH solution were then added to 10 mL plastic centrifuge tubes. After 20 s of vortexing, the mixtures were incubated at 37 °C for 20 min in a water bath. 2 mL of saturated NaCl solution were added to the mixtures, which were then extracted with 2 mL diethyl ether after mixing. The mixture was centrifuged at 1,500 rpm for 5 min and 1 mL of ether phase was collected and dried under vacuum. The residuum was dissolved with 200 μL methanol and filtered through a 0.45 μm membrane, and 10 μL of filtrate were collected for injection. Ten uniformly sized fruit were used for analysis, and the experiments were repeated three times.

References

- Alexander, L. & Grierson, D. Ethylene biosynthesis and action in tomato: a model for climacteric fruit ripening. *J Exp Bot* **53**, 2039–2055 (2002).
- Li, C. L., Jia, H. F., Chai, Y. M. & Shen, Y. Y. Abscisic acid perception and signaling transduction in strawberry: A model for non-climacteric fruit ripening. *Plant Signal & Behav* **6**, 1950–1953 (2011).
- Cherian, S., Figueroa, C. R. & Nair, H. 'Movers and shakers' in the regulation of fruit ripening: a cross-dissection of climacteric versus non-climacteric fruit. *J Exp Bot* **65**, 4705–4722 (2014).
- Shen, Y. Y. & Rose, J. K. C. ABA Metabolism and Signaling in Fleshy Fruits. In: *Abscisic Acid: Metabolism, Transport and Signaling* (Zhang D. P., ed.), pp. 271–286, Springer Science + Business Media Dordrecht (2015).
- Given, N. K., Venis, M. A. & Grierson, D. Hormonal regulation of ripening in the strawberry, a non-climacteric fruit. *Planta* **174**, 402–406 (1988).
- Chai, Y. M., Jia, H. F., Li, C. L., Dong, Q. H. & Shen, Y. Y. FaPYR1 is involved in strawberry fruit ripening. *J Exp Bot* **62**, 5079–5089 (2011).
- Jia, H. F. *et al.* Abscisic acid plays an important role in the regulation of strawberry fruit ripening. *Plant Physiol* **157**, 188–199 (2011).
- Jia, H. F. *et al.* Sucrose functions as a signal involved in the regulation of strawberry fruit development and ripening. *New Phytol* **198**, 453–465 (2013).
- Jia, H. F. *et al.* Type 2C protein phosphatase ABI1 is a negative regulator of strawberry fruit ripening. *J Exp Bot* **64**, 1677–1687 (2013).
- Daminato, M., Guzzo, F. & Casadoro, G. A SHATTERPROOF-like gene controls ripening in non-climacteric strawberries, and auxin and abscisic acid antagonistically affect its expression. *J Exp Bot* **64**, 3775–3786 (2013).
- Li, L. *et al.* Quantitative proteomic investigation employing stable isotope labeling by peptide dimethylation on proteins of strawberry fruit at different ripening stages. *J Proteomics* **94**, 219–239 (2013).
- Han, Y. *et al.* FaSnRK2.6, an ortholog of Open Stomata 1, is a Negative Regulator of Strawberry Fruit Development and Ripening. *Plant Physiol*. doi: 10.1104/pp.114.251314 (2015).
- Chai, Y. M. *et al.* Brassinosteroid is involved in strawberry fruit ripening. *Plant Growth Regulation* **69**, 63–69 (2013).
- Concha, C. M. Methyl jasmonate treatment induces changes in fruit ripening by modifying the expression of several ripening genes in *Fragaria chiloensis* fruit. *Plant Physiol Biochem* **70**, 433–444 (2013).
- Trainotti, L., Pavanello, A. & Casadoro, G. Different ethylene receptors show an increased expression during the ripening of strawberries: does such an increment imply a role for ethylene in the ripening of these non-climacteric fruits? *J Exp Bot* **56**, 2037–2046 (2005).
- Merchante, C. *et al.* Ethylene is involved in strawberry fruit ripening in an organ-specific manner. *J Exp Bot* **64**, 4421–4439 (2013).
- Csukasi, F. *et al.* Gibberellin biosynthesis and signalling during development of the strawberry receptacle. *New Phytol* **191**, 376–390 (2011).
- Manning, K. Isolation of a set of ripening-related genes from strawberry: their identification and possible relationship to fruit quality traits. *Planta* **205**, 622–631 (1998).
- Bombarely, A. *et al.* Generation and analysis of ESTs from strawberry (*Fragaria xananassa*) fruits and evaluation of their utility in genetic and molecular studies. *BMC Genomics* **11**, 503 (2010).
- Aharoni, A. & O'Connell, A. P. Gene expression analysis of strawberry achene and receptacle maturation using DNA microarrays. *J Exp Bot* **53**, 2073–2087 (2002).
- Bianco, L. *et al.* Strawberry proteome characterization and its regulation during fruit ripening and in different genotypes. *J Proteomics* **72**, 586–607 (2009).
- Xu, X. *et al.* High-throughput sequencing and degradome analysis identify miRNAs and their targets involved in fruit senescence of *Fragaria xananassa*. *PLoS One* **8**, e70959 (2013).
- Seymour, G. B. *et al.* A SEPALLATA gene is involved in the development and ripening of strawberry (*Fragaria x xananassa* Duch.) fruit, a non-climacteric tissue. *J Exp Bot* **62**, 1179–1188 (2011).
- Llop-Tous, I., Domínguez-Puigjaner, E. & Vendrell, M. Characterization of a strawberry cDNA clone homologous to calcium-dependent protein kinases that is expressed during fruit ripening and affected by low temperature. *J Exp Bot* **53**, 2283–2285 (2002).
- Schwab, W., Aharoni, A., Raab, T., Pérez, A. G. & Sanz, C. Cytosolic aldolase is a ripening related enzyme in strawberry fruits (*Fragaria x xananassa*). *Phytochemistry* **56**, 407–415 (2001).
- García-Limones, C. *et al.* Functional characterization of FaCCD1: a carotenoid cleavage dioxygenase from strawberry involved in lutein degradation during fruit ripening. *J Agric Food Chem* **56**, 9277–9285 (2008).
- Moyano-Cañete, E. *et al.* FaGAST2, a strawberry ripening-related gene, acts together with FaGAST1 to determine cell size of the fruit receptacle. *Plant Cell Physiol* **54**, 218–236 (2013).
- Aharoni, A. *et al.* Novel insight into vascular, stress, and auxin-dependent and -independent gene expression programs in strawberry, a non-climacteric fruit. *Plant Physiol* **129**, 1019–1031 (2002).
- Blanco-Portales, R. *et al.* Cloning, expression and immunolocalization pattern of a cinnamyl alcohol dehydrogenase gene from strawberry (*Fragaria x xananassa* cv. Chandler). *J Exp Bot* **53**, 1723–1734 (2002).
- Aharoni, A. *et al.* The strawberry FaMYB1 transcription factor suppresses anthocyanin and flavonol accumulation in transgenic tobacco. *Plant J* **28**, 319–332 (2001).
- Salvatierra, A., Pimentel, P., Moya-León, M. A. & Herrera, R. Increased accumulation of anthocyanins in *Fragaria chiloensis* fruits by transient suppression of FcMYB1 gene. *Phytochemistry* **90**, 25–36 (2013).
- Ring, L. *et al.* Metabolic interaction between anthocyanin and lignin biosynthesis is associated with peroxidase FaPRX27 in strawberry fruit. *Plant Physiol* **163**, 43–60 (2013).
- Schaart, J. G. *et al.* Identification and characterization of MYB-bHLH-WD40 regulatory complexes controlling proanthocyanidin biosynthesis in strawberry (*Fragaria x xananassa*) fruits. *New Phytol* **197**, 454–467 (2013).

34. Medina-Puche, L. *et al.* MYB10 plays a major role in the regulation of flavonoid/phenylpropanoid metabolism during ripening of *Fragaria x ananassa* fruits. *J Exp Bot* **65**, 401–417 (2014).
35. Posé, S. *et al.* Insights into the effects of polygalacturonase FaPG1 gene silencing on pectin matrix disassembly, enhanced tissue integrity, and firmness in ripe strawberry fruits. *J Exp Bot* **64**, 3803–3815 (2013).
36. Paniagua, C. *et al.* Fruit softening and pectin disassembly: an overview of nanostructural pectin modifications assessed by atomic force microscopy. *Ann Bot* **114**, 1375–1383 (2014).
37. Castillejo, C. *et al.* Pectin esterase gene family in strawberry fruit: study of FaPE1, a ripening-specific isoform. *J Exp Bot* **55**, 909–918 (2004).
38. Santiago-Doménech, N. *et al.* Antisense inhibition of a pectate lyase gene supports a role for pectin depolymerization in strawberry fruit softening. *J Exp Bot* **59**, 2769–2779 (2008).
39. Trainotti, L., Spolaore, S., Pavanello, A., Baldan, B. & Casadoro, G. A novel E-type endo- β -1,4-glucanase with a putative cellulose-binding domain is highly expressed in ripening strawberry fruits. *Plant Mol Biol* **40**, 323–332 (1999).
40. Woolley, L. C., James, D. J. & Manning, K. Purification and properties of an endo- β -1,4-glucanase from strawberry and down-regulation of the corresponding gene, cell1. *Planta* **214**, 11–21 (2001).
41. Molina-Hidalgo, F. J. *et al.* The strawberry (*Fragaria x ananassa*) fruit-specific rhamnogalacturonate lyase 1 (FaRGLyase1) gene encodes an enzyme involved in the degradation of cell-wall middle lamellae. *J Exp Bot* **64**, 1471–1483 (2013).
42. Martínez, G. A., Chaves, A. R. & Civello, P. M. β -xylosidase activity and expression of a beta-xylosidase gene during strawberry fruit ripening. *Plant Physiol Biochem* **42**, 89–96 (2004).
43. Bustamante, C. A., Rosli, H. G., Añón, M. C., Civello, P. M. & Martínez, G. A. β -Xylosidase in strawberry fruit: Isolation of a full-length gene and analysis of its expression and enzymatic activity in cultivars with contrasting firmness. *Plant Sci* **171**, 497–504 (2006).
44. Trainotti, L., Spinello, R., Piován, A., Spolaore, S. & Casadoro, G. β -Galactosidases with a lectin-like domain are expressed in strawberry. *J Exp Bot* **52**, 1635–1645 (2001).
45. Dotto, M. C., Martínez, G. A. & Civello, P. M. Expression of expansin genes in strawberry varieties with contrasting fruit firmness. *Plant Physiol Biochem* **44**, 301–307 (2006).
46. Mut, P. *et al.* A fruit-specific plasma membrane aquaporin subtype PIP1 is regulated during strawberry (*Fragaria x ananassa*) fruit ripening. *Physiol Plant* **132**, 538–551 (2008).
47. Alleva, K. *et al.* Cloning, functional characterization, and co-expression studies of a novel aquaporin (FaPIP2) of strawberry fruit. *J Exp Bot* **61**, 3935–3945 (2010).
48. Yaneff, A. *et al.* Heteromerization of PIP aquaporins affects their intrinsic permeability. *Proc Natl Acad Sci USA* **111**, 231–236 (2014).
49. Aharoni, A. *et al.* Identification of the SAAT gene involved in strawberry flavor biogenesis by use of DNA microarrays. *Plant Cell* **12**, 647–662 (2000).
50. Yahyaoui, F. E. *et al.* Molecular and biochemical characteristics of a gene encoding an alcohol acyl-transferase involved in the generation of aroma volatile esters during melon ripening. *Eur J Biochem* **269**, 2359–2366 (2002).
51. Beekwilder, J. *et al.* Functional characterization of enzymes forming volatile esters from strawberry and banana. *Plant Physiol* **135**, 1865–1878 (2004).
52. González, M. *et al.* Aroma development during ripening of *Fragaria chiloensis* fruit and participation of an alcohol acyltransferase (FaAAT1) gene. *J Agric Food Chem* **57**, 9123–9132 (2009).
53. Cumplido-Laso, G. *et al.* The fruit ripening-related gene FaAAT2 encodes an acyl transferase involved in strawberry aroma biogenesis. *J Exp Bot* **63**, 4275–4290 (2012).
54. Ponce-Valadez, M. & Watkins, C. B. Fermentation and malate metabolism in response to elevated CO₂ concentrations in two strawberry cultivars. *Physiol Plant* **134**, 121–133 (2008).
55. Wein, M. *et al.* Isolation, cloning and expression of a multifunctional O-methyltransferase capable of forming 2,5-dimethyl-4-methoxy-3(2H)-furanone, one of the key aroma compounds in strawberry fruits. *Plant J* **31**, 755–765 (2002).
56. Lunkenbein, S. *et al.* Up- and down-regulation of *Fragaria x ananassa* O-methyltransferase: impacts on furanone and phenylpropanoid metabolism. *J Exp Bot* **57**, 2445–2453 (2006).
57. Zorrilla-Fontanesi, Y. *et al.* Genetic analysis of strawberry fruit aroma and identification of O-methyltransferase FaOMT as the locus controlling natural variation in mesifurane content. *Plant Physiol* **159**, 851–870 (2012).
58. Aharoni, A. *et al.* Gain and loss of fruit flavor compounds produced by wild and cultivated strawberry species. *Plant Cell* **16**, 3110–3131 (2004).
59. Chambers, A. H. *et al.* Identification of a strawberry flavor gene candidate using an integrated genetic-genomic-analytical chemistry approach. *BMC Genomics* **15**, 217 (2014).
60. Aragüez, I. *et al.* Eugenol production in achenes and receptacles of strawberry fruits is catalyzed by synthases exhibiting distinct kinetics. *Plant Physiol* **163**, 946–958 (2013).
61. Lunkenbein, S. *et al.* Cinnamate metabolism in ripening fruit. Characterization of a UDP-glucose:cinnamate glucosyltransferase from strawberry. *Plant Physiol* **140**, 1047–1058 (2006).
62. Xiao-Jiao, H., Yang-Dong, W., Yi-Cun, C., Li-Yuan, L. & Qing-Ke, W. Transcriptome sequencing and expression analysis of terpenoid biosynthesis genes in *Litsea cubeba*. *Plos one* **8**, 1–14 (2013).
63. Grabherr, M. G. *et al.* Trinity: reconstructing a full-length transcriptome without a genome from RNA-Seq data. *Nat Biotechnol* **29**, 644–652 (2011).
64. Sheng, X. & Liu, Y. Theoretical study of the catalytic mechanism of E1 subunit of pyruvate dehydrogenase multienzyme complex from *Bacillus stearothermophilus*. *Biochemistry* **52**, 8079–8093 (2013).
65. Ozden, O. *et al.* SIRT3 deacetylates and increases pyruvate dehydrogenase activity in cancer cells. *Free Radic Biol Med* **76**, 163–172 (2014).
66. Mayers, R. M., Leighton, B. & Kilgour, E. PDH kinase inhibitors: a novel therapy for Type II diabetes? *Biochem Soc Trans* **33**, 367–370 (2005).
67. Sun, J. H. *et al.* New evidence for the role of ethylene in strawberry fruit ripening. *Journal of Plant Growth Regulation* **32**, 461–470 (2012).
68. Merchante, C. *et al.* Ethylene is involved in strawberry fruit ripening in an organ-specific manner. *J Exp Bot* **64**, 4421–4439 (2013).
69. Wang, Y., Xu, F., Feng, X. & MacArthur, R. L. Modulation of *Actinidia arguta* fruit ripening by three ethylene biosynthesis inhibitors. *Food Chem* **173**, 405–4013 (2015).
70. Mingying, L. *et al.* Transcriptome sequencing and de novo analysis for bamboo using the illumina platform. *Plos one* **7**, 1–11 (2012).
71. Wang, Z. *et al.* De novo assembly and characterization of root transcriptome using Illumina paired-end sequencing and development of cSSR markers in sweetpotato (*Ipomoea batatas*). *BMC Genomics* **11**, 726 (2010).
72. Kent, W. J. BLAT—The BLAST-Like Alignment Tool. *Genome Res* **12**, 656–664 (2002).
73. Altschul, S. F. *et al.* Gapped BLAST and PSI-BLAST: a new generation of protein database search programs. *Nucleic Acids Res* **25**, 3389–3402 (1997).
74. Conesa, A., Götz, S., García-Gómez, J. M., Terol, J. & Talón, M. Blast2GO: a universal tool for annotation, visualization and analysis in functional genomics research. *Bioinformatics* **21**, 3674–3676 (2005).
75. Conesa, A. & Götz, S. Blast2GO: A comprehensive suite for functional analysis in plant genomics. *Int J Plants Genom.* doi: 10.1155/2008/619832 (2008).

76. Moriya, Y. *et al.* KAAS: an automatic genome annotation and pathway reconstruction server. *Nucleic Acids Res* **35**, 182–185 (2007).
77. Karp, P. D., Paley, S. & Romero, P. The pathway tools software. *Bioinformatics* **18**, 225–232 (2002).
78. Kanehisa, M., Goto, S., Kawashima, S., Okuno, Y. & Hattori, M. The KEGG resource for deciphering the genome. *Nucleic Acids Res* **32**, 277–280 (2004).
79. Ben, L. & Salzberg, S. L. Fast gapped-read alignment with Bowtie 2. *Nature methods* **9**, 357–359 (2012).
80. Mortazavi, A., Williams, B. A., McCue, K., Schaeffer, L. & Wold, B. Mapping and quantifying mammalian transcriptomes by RNA-Seq. *Nat Meth* **5**, 621–628 (2008).
81. Benjamini Yoav, Y. D. The control of the false discovery rate in multiple testing under dependency. *The annals of statistics* **29**, 1165–1188 (2001).

Acknowledgements

This work was supported the China National Science Foundation (Project 31471837, 31272144, 41473004) and the National Key Technology Supported Program of China (Project 2011BAD32B03), the Project of Construction of Innovative Teams and Teacher Career Development for Universities and Colleges under Beijing Municipality (Grant No. IDHT20140509), Beijing Training Project for the Leading Talents in S & T (grant No. LIRC201612), and Beijing Municipal Education Commission (grant No. CEFF-PXM2016-014207-000038).

Author Contributions

Qing-Hua Wang and Cheng Zhao performed the experiments; Miao Zhang and Yu-Zhong Li analyzed the data; Jia-Xuan Guo and Yuan-Yue Shen designed and wrote the article.

Additional Information

Supplementary information accompanies this paper at <http://www.nature.com/srep>

Competing financial interests: The authors declare no competing financial interests.

How to cite this article: Wang, Q.-H. *et al.* Transcriptome analysis around the onset of strawberry fruit ripening uncovers an important role of oxidative phosphorylation in ripening. *Sci. Rep.* **7**, 41477; doi: 10.1038/srep41477 (2017).

Publisher's note: Springer Nature remains neutral with regard to jurisdictional claims in published maps and institutional affiliations.



This work is licensed under a Creative Commons Attribution 4.0 International License. The images or other third party material in this article are included in the article's Creative Commons license, unless indicated otherwise in the credit line; if the material is not included under the Creative Commons license, users will need to obtain permission from the license holder to reproduce the material. To view a copy of this license, visit <http://creativecommons.org/licenses/by/4.0/>

© The Author(s) 2017